Article, Published Version

Dufek, Tanja

Backscatter Analysis of Multi-beam Sonar Data in the Area of the Valdivia Fracture Zone

Hydrographische Nachrichten

Backscatter Analysis of Multi-beam Sonar Data in the Area of the Valdivia Fracture Zone

An article by *Tanja Dufek*

For this master thesis multi-beam echo-sounder (MBES) data was acquired with a Simrad Kongsberg EM 120 (12 kHz) on RV »Sonne« cruise SO213-1 (organised by the Alfred Wegener Institute, Bremerhaven) in the deep-sea environment of the Valdivia Fracture Zone. This dataset was used to examine the Geocoder implementation in CARIS HIPS and SIPS 7.1 and QPS Fledermaus 7.3 for MBES backscatter processing, mosaicking, and automatic sediment classification. Furthermore, the obtained angle-invariant MBES backscatter data was investigated for its potential to allow conclusions on the sediment type distribution throughout the surveyed area.

Backscatter analysis | QPS Fledermaus | CARIS HIPS and SIPS | Geocoder | Valdivia Fracture Zone

1 Introduction

MBES transmit a large number of acoustic signals in different grazing angles grouped in a fan towards the seafloor. Reaching the sediments, three different processes occur: one part of the signal is reflected in symmetrical direction (specular reflection), a second part is scattered in all directions, and a third part penetrates the seabed (Fig. 1). The scattering of the signal towards the sonar is called backscatter. By measuring the duration between transmission of the signal and reception of the backscattered wave, the water depth can be calculated by the echo-sounder based on the determined water sound velocity.

The backscatter strength varies with the incident signal (e.g., angle, frequency) and the seafloor characteristics. The influencing seafloor characteristics include seafloor roughness at scales comparable to the sonar's wavelength and intrinsic properties of the seafloor (Fig. 2) (Blondel et al. 1997).

Some MBES do not only measure the travel time of the acoustic wave for depth determination but also record the intensity of the returned signal and therefore the backscatter strength. Multi-beam backscatter information has been the subject of research in the last decades. The aim is to analyse the backscattered response of the seafloor in order to obtain sediment properties (e.g., grain size). Geocoder is a software toolkit developed by Dr. Fonseca (Fonseca et al. 2005) and was implemented into CARIS HIPS and SIPS and Fledermaus. These Geocoder implementations were used and evaluated for MBES backscatter processing, mosaicking, and sediment classification for the recorded dataset.

2 Data acquisition and processing

The dataset used for backscatter analysis was collected on the RV »Sonne« cruise SO213 leg 1 in January 2011 in the area of the Valdivia Fracture Zone about 950 km west of the Chilean coast and 750 km south of Valparaiso. The cruise was organised by the Alfred Wegener Institute in Bremerhaven and led by Prof. Dr. Ralf Tiedemann. A Simrad EM 120 from Kongsberg that operates at a frequency of 12 kHz was used. An area of 53 × 25 km² was systematically mapped with 14 profiles arranged in different directions (Fig. 3). The water depth ranges from 2,091 m to 4,779 m.

Author

Tanja Dufek works at Fugro OSAE in Bremen as Offshore Data Processor.

Contact:

tanja.dufek@yahoo.de

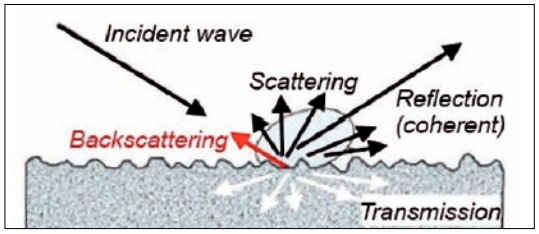

Fig. 1 (left): Reflection, transmission, and scattering of an incident wave by the seafloor (Lurton 2010)

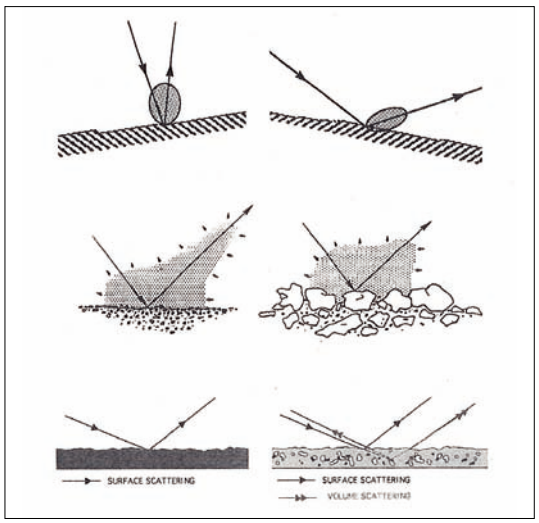

Fig. 2 (left): Influences of seafloor backscattering (Blondel et al. 1997)

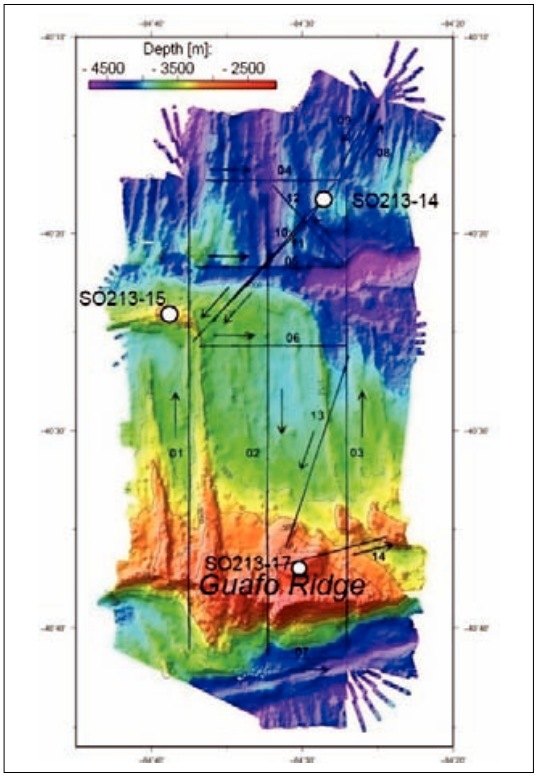

Fig. 3 (right): MBES data and locations of sediment samples (white dots). The profiles used for backscatter analysis (black lines) are depicted as well as their direction of recording

The morphology of the survey area is characterised by strong morphological changes caused by the tectonic activity of the nearby spreading ridge of the Chile Rise. Furthermore, three surface sediment samples were taken in the study area for ground-truthing with a multicorer. The sediment grain size was measured with the laser particle sizer Beckman Coulter LS 200 at the MARUM, University of Bremen.

Blunders were removed from the MBES data before processing and analysing the backscatter information with Geocoder in CARIS HIPS and SIPS and Fledermaus.

3 Method

Geocoder is a software toolkit developed by Dr. Luciano Fonseca and licensed by the University of New Hampshire. It processes raw backscatter data, creates backscatter mosaics, and performs an Angular Range Analysis (ARA) for remote estimation of seafloor properties (Fig. 4). It is a stand-alone software but was recently implemented into different software like CARIS HIPS and SIPS and Fledermaus. In the following the general processing and analysis steps are briefly outlined.

3.1 Radiometric and geometric corrections

Before the backscatter data can be mapped or analysed, different radiometric and geometric corrections need to be applied to the dataset. Radiometric corrections reduce the effects of perturbation during data acquisition and data transfer to obtain the best estimate of the backscatter strength returned from the seafloor. Amongst others they include a time varying gain (TVG) correction, which removes the automatically applied gain during data acquisition, corrections for acquisition geometry, and a beam pattern correction to remove systematic hardware and sediment artefacts.

Geometric distortions occur due to the fact that the data is sampled in time (time series format of EM 120). They are corrected by a slant-range correction based on bathymetric measurements that transforms the slant-range time samples into horizontal distances to the acoustic source.

3.2 Mosaic blending

After applying radiometric and geometric corrections, corrected angular responses are obtained. Since these depend on the incident angle of the beam (values close to nadir are higher than at the outer swath), an angular varying gain (AVG) correction is applied to obtain angle-invariant data. This way a homogeneous seafloor image can be generated without artefacts in along-track direction. For mapping overlapping samples, a weighted interpolation is applied according to a quality factor, which is assigned to the intensity values and corresponds to the incidence angle. Values close to nadir and at the outer edge of the swath get lower values than in the mid-range.

3.3 Angular Range Analysis

The Angular Range Analysis (ARA) employs the fact that each sediment type has its unique angular response. The backscatter variation with respect to the grazing angle is a function of the seafloor properties. For an estimation of the seafloor characteristics, the inversion of an acoustic model is used.

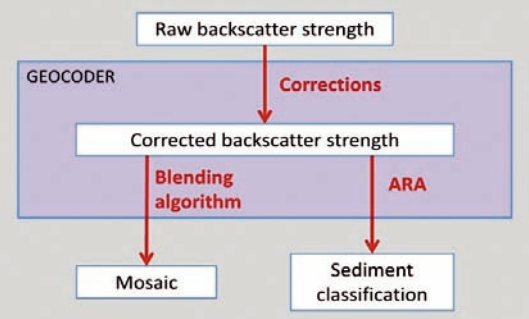

Fig. 4: Schematic representation of Geocoder functionality

Tab. 1: Comparison of possible settings and data formats of Geocoder in CARIS HIPS and SIPS and Fledermaus

	Product:	CARIS HIPS and SIPS	Fledermaus (FMGeocoder Toolbox)
	Version:	7.1.1	7.3.1
	Import formats:	over 40 formats	GSF, XTF, GSF/XTF Pair, GSF/S7K Pair, Kongsberg (*.all)
Backscatter Processing	**Backscatter format:**	beam average, beam time series, time series (side-scan)	beam average, beam time series, time series (side-scan)
	Backscatter corrections (user settings possible):	auto gain, auto TVG, anti-aliasing, beam pattern, AVG, despeckle	TX/RX correction, AVG, beam pattern
Mosaicking	**Mosaic blending algorithm:**	overwrite, shine through, underlay, auto-seam (pixel chosen by weight), full blend (weighted interpolation)	blend (not weighted), weighted methods: no nadir if possible 1, no nadir if possible 2
	Mosaic export formats:	TIFF, GeoTIFF, ASCII	GeoTIFF, surface (z, xyz, ArcView grid (.asc), binary heights (.bin), GMT grid (.grd), floating point, Fledermaus format (.sd)
	Improvement of mosaic appearance:	changes in brightness and contrast, histogram alignement	histogram stretching
ARA	**Acoustic model:**	Jackson model or Biot theory	Jackson model
	Patch size:	half a swath/user setting	half a swath/30 pings
	ARA result presentation:	patch based	surface based or patch based
	ARA export formats:	ASCII file (patch based)	Surface: GeoTIFF, surface, ArcGIS format, SD/patch: ASCII ARA, point ARA Object (.sd)

4 Geocoder implementation in CARIS and Fledermaus – Comparison and results

As the same algorithms of Geocoder were implemented into CARIS HIPS and SIPS (Mosaic Editor, Geocoder Engine) and Fledermaus (FMGeocoder Toolbox), the applied corrections and computations are very similar in both software packages and no large differences are expected. However, slight differences concerning the implementation are recognisable. In Tab. 1 possible settings and data formats for Geocoder in CARIS and Fledermaus are listed. In the following, the Geocoder implementation of both software products is compared based on the results of the recorded deep-sea dataset.

4.1 Backscatter processing

In CARIS HIPS and SIPS and Fledermaus some of the corrections are hidden and cannot be controlled by the user. In comparison, CARIS allows slightly more involvement of the user with a larger number of unhidden corrections and possible settings. The workflow in CARIS includes the intermediate step of GeoBaR (Georeferenced Backscatter Raster), representing the corrected backscatter data for one line.

The applied corrections showed satisfying results in both software products, but the removal of topographic effects did not fully succeed in either software, and artefacts caused by morphology are still visible in the angular response (Fig. 5).

4.2 Mosaicking

Both software products offer different blending algorithms for mosaicking (Tab. 1). »Full blend« of CARIS and »no nadir if possible« of Fledermaus correspond to the weighted interpolation approach of Geocoder. A comparison of mosaics created with these methods showed the best result (low nadir and seam artefacts) for both implementations. Comparing the results with each other, the »full blend« algorithm in CARIS showed nadir and systematic artefacts, whereas the result of Fledermaus (»no nadir if possible 2«) seems to generate a more homogeneous image in areas of overlapping profiles for the investigated dataset (Fig. 6). Fledermaus displays more mosaic statistics if required by the user and offers a larger variety of mosaic export formats (Tab. 1).

4.3 Angular Range Analysis

The ARA is applied to single patches of the dataset. The width of such a patch corresponds to half a swath width. Its length is set to 30 consecutive pings in Fledermaus, whereas this value can be defined by the user in CARIS. The angular response of one patch is averaged and analysed based on the Jackson model (Jackson et al. 1998). In addition, the grain size table can be edited by the user and also the Biot theory (Biot 1956) can be used for the inverse modelling of the ARA in CARIS. In contrast, the export possibilities for ARA results as provided by Fledermaus are more numerous than in CARIS.

In Tab. 2 the grain size measurements using a laser particle sizer Beckman Coulter LS 200 are listed. At location SO213-14 manganese nodules with a diameter of 2 to 3 cm were recovered on clayey sediment.

Location	Water depth [m]	Grain size [µm]	Sediment type
SO213-14	4,050	3.58	Manganese nodules (Gravel)/Clay
SO213-15	3,246	98.13	Very fine sand/ Coarse silt
SO213-17	2,561	130.7	Fine sand/ Very fine sand

Tab. 2: Grain size at the sediment sampling locations of the investigation area

In CARIS and Fledermaus the ARA results can be depicted with coloured indicators for sediment properties like in Fig. 7. Different grain sizes are presented by colours for each patch. Fledermaus also offers a surface representation of the ARA results besides the patch based representation. In CARIS confidence levels are given for each ARA sediment classification. These confidence levels are represented by the size of the indicator in Fig. 7 (left).

Geocoder offers the possibility to assign a sediment class to the beam pattern file (ground-truthing). This was done at each sediment sampling location and the different ARA results were compared. When comparing the ARA results of CARIS and Fledermaus different beam pattern correction settings yield plausible results. When SO213-17 is used in CARIS as ground-truthing location (Fig. 7, left) the north and south of the investigation area are classified as gravel and the intermediate part as sand. This corresponds to the predominant high backscatter strength in the north and south and the in comparison lower backscatter strength in the middle of the survey area. A similar but not as distinctive result is obtained when SO213-14 is used as ground-truthing location in Fledermaus

Fig. 5 (top): Visualisation of remaining bathymetric artefacts in the angular response. The turquoise line indicates the location of the angular response (top left) and the image in the top right corner shows the cross section of its corresponding bathymetry. Angular response of the corresponding patch in CARIS (bottom left) and Fledermaus (bottom right). Blue circles point out locations where the seafloor slope is oriented towards the echo-sounder. These areas are apparent also in the angular responses

Fig. 6 (bottom): Mosaics created in CARIS with the »full blend« algorithm (left), and in Fledermaus with »no nadir if possible 2« (right). Yellow lines indicate the ship track

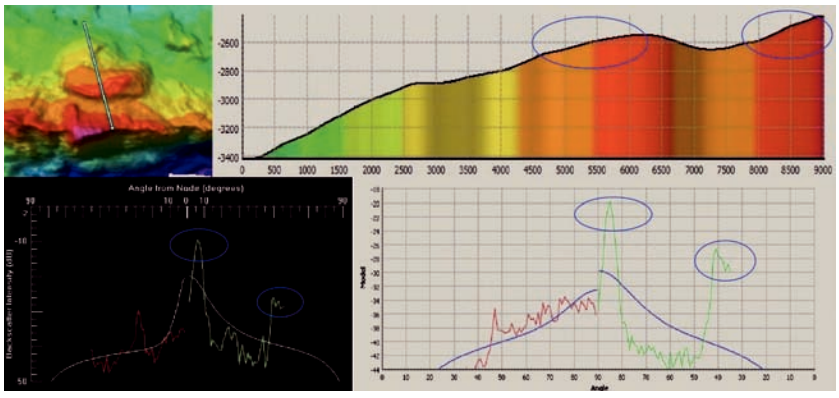

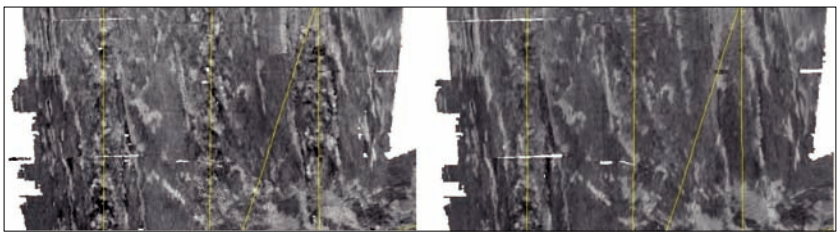

(Fig. 7, right). Beyond that, ARA results with appliance of no beam pattern correction and a beam pattern correction without ground-truthing were investigated but did not seem reliable.

The different settings used in CARIS and Fledermaus resulting in the most plausible sediment classifications, are probably due to the deep-sea environment of the investigated dataset. The deep-sea environment with great water depths lead to large patch sizes analysed by the ARA. A very important requirement for a robust automatic sediment classification is that there should be only one sediment type within a patch. The larger the patches, the greater the possibility of containing different sediment types. Furthermore, the dataset was recorded close to a tectonic active area and therefore shows strong bathymetric variations. Due to the imperfect topographic correction, the angular responses are falsified, and in areas with strong depth variations, estimates of sediment types are unreliable. Therefore deep-sea data is not highly suited for a patch-based ARA.

5 Backscatter Analysis

The variation of sediment grain size is the main contributor to variations in backscatter strength. Generally, the backscatter intensities increase with grain size, so that softer sediments like clay exhibit smaller backscatter strengths than when coarser sediments with low water content are predominant.

When examining the angle-invariant data of the investigation area (Fig. 8, left), the topographic influence is visible in the backscatter mosaic as morphologic features can clearly be recognised. Even though, three areas can broadly be separated according to their mean backscatter strength (Fig. 8): the northern (A) and southern part (C) show high backscatter values whereas the intermediate region (B) shows lower values.

Area A corresponds to the bathymetric deeper area with depths of more than 4,000 m and strong fissured relief. In this area manganese nodules were found in the surface sediment sample. The general high backscatter response (-19 dB) throughout the area indicates the presence of manganese nodules in area A. This assumption is supported by the large water depth, as this is an important condition for the creation of manganese nodules.

Area B is characterised by lower backscatter strengths of around -35 dB. Two of the sediment samples were recovered in this area and it can be assumed, that the predominant grain size would be in the range of silt-to-sand throughout this area.

The southern area C of the dataset shows backscatter values around -20 dB. It corresponds to the southern scarp of the Guafo Ridge and the adjacent fault in the south of the ridge. The presence of manganese nodules can be excluded as possible cause for the mean high backscatter response because of the relative shallow water depth. The southern slope of the Guafo Ridge is very steep (20°) so that sediments cannot accumulate easily and slides are enforced. Basement outcrops are therefore very likely in this part and would explain the high backscatter response as result of a high impedance contrast.

Since the EM 120 had not been calibrated, absolute backscatter values were not determined, and can therefore not directly be matched with other backscatter measurements of different investigations. However, the relative values between two sediment types (e.g., 15 dB between basement and sandy sediment) correspond to examples in literature, where similar backscatter contrasts are reported as in the dataset investigated here.

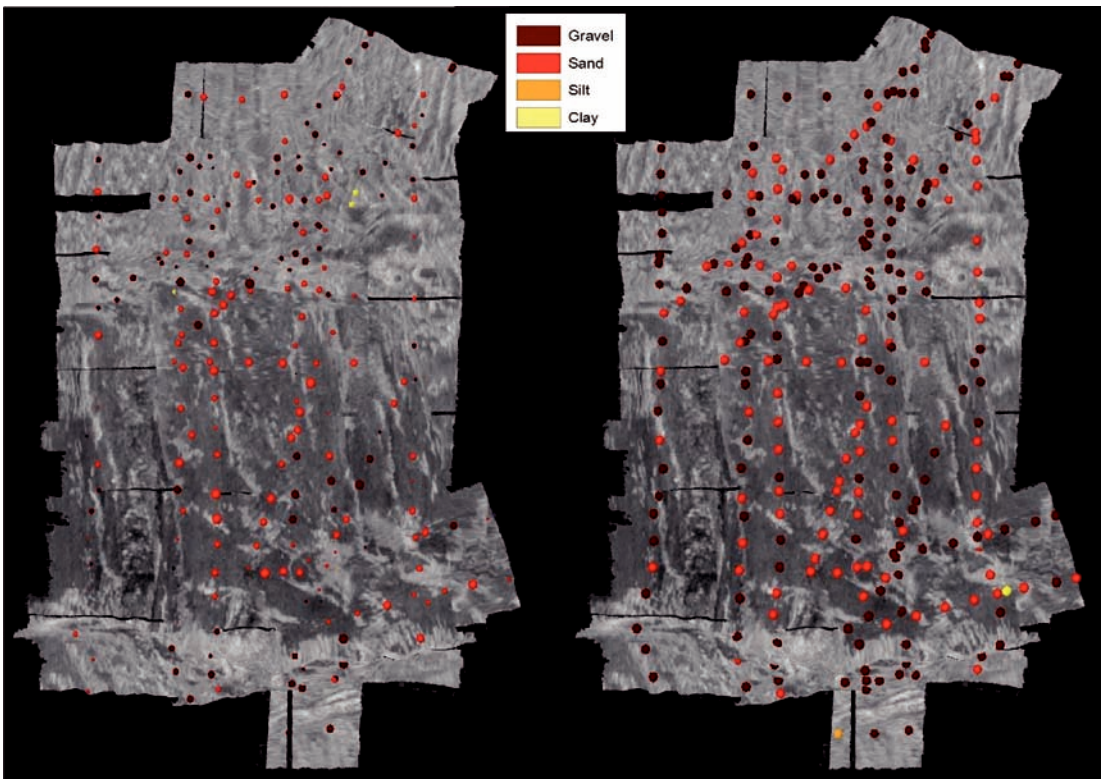

Fig. 7: Mosaics created and visualised in Fledermaus with high backscatter values represented white and low values depicted black. ARA results of CARIS with SO213-17 as ground-truthing location (left) and Fledermaus with ground-truthing at SO213-14 (right)

6 Conclusions

The objectives of this thesis were two-fold: on the one hand, the Geocoder implementation in CARIS HIPS and SIPS and Fledermaus was examined for MBES backscatter processing and automatic sediment classification of data acquired in a deep-sea environment. On the other hand, the obtained angle-invariant MBES backscatter data was investigated for its potential to allow conclusions on the sediment type distribution in the survey area.

The applied corrections showed satisfying results in both software products in general, but the removal of topographic influences did not fully succeed in either software. As a result, topographic features are visible in the angle-invariant data of the mosaics and automatic sediment classification by the ARA is affected. The blending algorithm in CARIS showed nadir artefacts, whereas computed mosaics in Fledermaus depicted more homogeneous results. Both applications showed seam-affects in areas with a larger amount of overlapping profiles.

The automatic sediment classification by an ARA with inverse modelling is not trivial since sediment structures often consist of complex compositions of different particles like pore water, organic material, and probably gas. Acoustic models cannot account for all physical processes. Deep-water environments complicate the patch-based ARA due to the large swath width. This was crucial for the investigated dataset as it is characterised by strong bathymetric variation. It was observed that the ARA results were influenced by the seafloor topography since its effect could not be completely removed from the angular responses. However, some of the obtained results of the ARA correspond to the expected sediment distribution, even though the dataset was not perfectly suited for an ARA. Ground-truthing showed to be very important for a more secure ARA and for an evaluation of its results.

In conclusion, both implementations have hidden computations, but the Geocoder implementation of Fledermaus has a stronger »black box« character than the one in CARIS. Neither software manual explains the algorithms precisely. But in comparison, CARIS provides the user with more information on the evaluation of results (e.g., images of mosaic weight distribution, confidence levels assigned to ARA results, or implementation of the intermediate processing step of GeoBaR generation). The advantage of Fledermaus in contrast lies in a more robust computation routine and a larger variety of export formats yielding a larger number of result representations.

Even though topographic artefacts were visible in the data, an estimate of the sediment distribution was possible. A high abundance of manganese nodules can be assumed for the northern part of the investigated area, whereas the intermediate part is covered by silt-to-sandy sediments. At the very southern part of the dataset basement outcrops could be established.

In conclusion, Geocoder is a promising processing and analysis tool for MBES backscatter data and can also be employed for datasets acquired in deep-sea environments. A new ARA approach that includes clustering of areas with similar angular responses instead of using patches of consecutive pings (Fonseca et al. 2007) seems to promise an improvement of automatic sediment classification, particularly for deep-sea environments. □

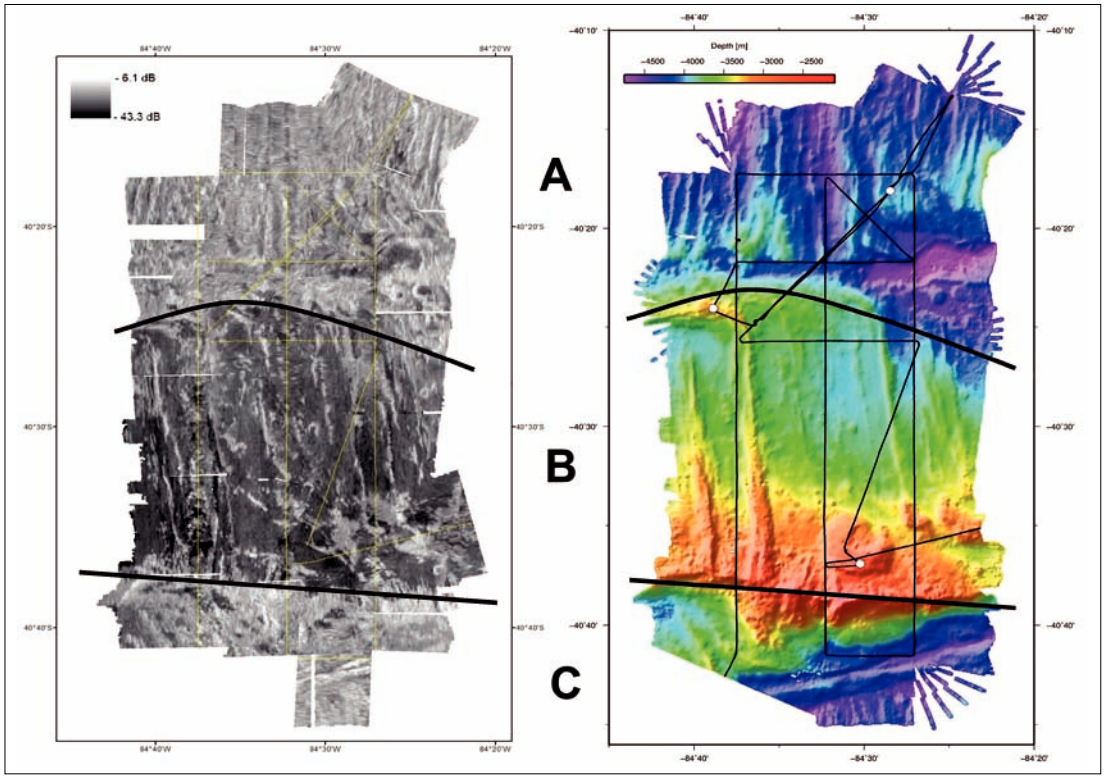

Fig. 8: Mosaic (left) and bathymetric chart with track plot (right) of the investigation area divided into northern (A), intermediate (B), and southern area (C) by mean backscatter strength. White dots indicate the sediment sampling locations

References

Biot, M.A. (1956): Theory of propagation of elastic waves in a fluid-saturated porous solid. I. Low-frequency range. Journal of the Acoustic Society of America, 28(2), pp. 168–178

Blondel P., B.J. Murton (1997): Handbook of seafloor sonar imagery. 1st Edition; John Wiley and Sons, Praxis Publishing, Chichester

Fonseca, L., B. Calder (2005): Geocoder: An efficient backscatter map constructor; Proceedings of the U.S. Hydrographic Conference 2005, San Diego (CA), USA

Fonseca, L., B. Calder (2007): Clustering acoustic backscatter in the angular response space; Proceedings of the U.S. Hydrographic Conference 2007, Norfolk (VA), USA

Jackson, D., A.N. Ivakin (1998): Scattering from elastic sea beds: First-order theory. Journal of the Acoustic Society of America, 103(1), pp. 336–345

Lurton, X. (2010): An introduction to underwater acoustics – principles and application. 2nd Edition; Springer, Berlin, Heidelberg

Acknowledgements

I would like to thank my supervisors Prof. Dr. Delf Egge and Prof. Dr. Hans Werner Schenke for their guidance and support of this thesis. Furthermore, I would like to thank the Alfred Wegener Institute, Prof. Dr. Ralf Tiedemann, and all participants of cruise SO213-1.